

See discussions, stats, and author profiles for this publication at: <https://www.researchgate.net/publication/281959595>

# Characterization and Sodium Sorption Capacity of Biochar and Activated Carbon Prepared from Rice Husk

Article in *Journal of Agricultural Science and Technology* · July 2015

CITATIONS

84

READS

2,080

4 authors, including:



[Manouchehr Heidarpour](#)

Isfahan University of Technology

114 PUBLICATIONS 1,953 CITATIONS

[SEE PROFILE](#)



[Sayed-Farhad Mousavi](#)

Semnan University

185 PUBLICATIONS 3,506 CITATIONS

[SEE PROFILE](#)



[Afyuni Majid](#)

Isfahan University of Technology

185 PUBLICATIONS 5,604 CITATIONS

[SEE PROFILE](#)

## Characterization and Sodium Sorption Capacity of Biochar and Activated Carbon Prepared from Rice Husk

R. Rostamian<sup>1</sup>, M. Heidarpour<sup>1\*</sup>, S. F. Mousavi<sup>2</sup>, and M. Afyuni<sup>3</sup>

### ABSTRACT

Biochar and activated carbon, as carbon-rich porous materials, have wide environmental applications. In the present research, rice husk (RH) was used for preparation of biochar at 400, 600, and 800 °C under simple pyrolysis, physically-activated carbon with water steam, chemically-activated carbon with potassium hydroxide (KOH), and physiochemically-activated carbon with KOH and steam. Physical and chemical properties of biochar and activated carbons were characterized using nitrogen adsorption-desorption isotherm, Fourier transform, infra-red analysis, and Boehm method. The results showed that carbonization temperature and activation agents had significant effects on the characteristics of the samples. Activated carbon produced by KOH activation had the highest surface area ( $2201 \text{ m}^2 \text{ g}^{-1}$ ) and total pore volume ( $0.96 \text{ cm}^3 \text{ g}^{-1}$ ). High concentration of sodium (Na) is an important limiting factor to reuse poor quality water resources in arid and semiarid regions. The sorption capacity of biochars and activated carbons was investigated by performing batch sorption experiments using Na as adsorbate. Na sorption was increased with increasing surface area and pore volume. The highest Na sorption capacity of  $134.2 \text{ mg g}^{-1}$  was achieved by the KOH activated carbon, which has the highest surface area and pore volume. The kinetic data were well-fitted to pseudo-first order and intra-particle diffusion models.

**Keywords:** Adsorbent, Diffusion models, Nitrogen isotherm, Physiochemical characteristics, Sorption isotherm.

### INTRODUCTION

In arid and semiarid regions of the world, demand for clean and fresh water is increasing because of population growth and industrial development. The scarcity of fresh water resources has impelled humans to reuse poor quality water such as saline and brackish water or drainage water. Salinity can negatively impact plants through osmotic, nutritious, and toxic stresses (Mousavi *et al.*, 2009). Sodium (Na) is the major cation causing salinity and high concentration of Na is an important limiting factor to reuse saline water. Various

techniques have been used for water desalination. These techniques are usually not economical due to their energy dependence and high costs, especially for agricultural purposes, which is the biggest water consumer in the world. Therefore, pretreatment of saline water before applying these methods can be used to reduce desalination costs.

Utilizing adsorbents, as an economical method, is usual for removal of different ionic species from water. Hence, finding inexpensive and efficient adsorbents for removing ions causing salinity from water resources is an important issue. Gasco *et al.*

<sup>1</sup> Department of Water Engineering, Isfahan University of Technology, Isfahan 84156-83111, Islamic Republic of Iran.

\* Corresponding author, email: Heidar@cc.iut.ac.ir

<sup>2</sup> Department of Civil Engineering, Semnan University, Semnan 35131-19111, Islamic Republic of Iran.

<sup>3</sup> Department of Soil Science, Isfahan University of Technology, Isfahan 84156-83111, Islamic Republic of Iran.



(2005) introduced carbon-based adsorbents prepared from sewage sludge, as inexpensive acceptable materials, to remove  $\text{Na}^+$ ,  $\text{K}^+$ ,  $\text{Ca}^{2+}$ , and  $\text{Mg}^{2+}$  cations from saline water. Aghakhani *et al.* (2011) considered dual adsorbents (combinations of peat, activated carbon, zeolite, cationic resins and anionic resins) in removal of salinity ions from drainage water. This study confirmed that application of cationic resin with peat had the highest ability to desalinate drainage water as compared to other adsorbents.

Biochars are low-cost carbon-rich porous materials obtained by pyrolysis of organic residues. The production of biochar by pyrolysis is a carbonization process in which the content of carbon increases with temperature, accompanied by simultaneous decrease in oxygen and hydrogen content. Biochars have many positive properties such as large surface area, high porosity and active functional groups, which are highly influenced by the source of feedstock and the preparation process (Jiang *et al.*, 2012). Biochar has been evaluated widely in water treatment applications for removing various contaminants, including heavy metals, pesticides, and organic compounds (Kolodynska *et al.*, 2012; Zhang *et al.*, 2011).

Activated carbon is an excellent adsorbent which has been used extensively for removal of various pollutants from gaseous and liquid phases (Lu *et al.*, 2012; Pehlivan and Cetin, 2008). Activated carbon can be produced by activation of biochar. Activation usually improves the adsorption capacity of biochar in order to greatly increase its porosity and surface area. Activation can be carried out by either physical methods or chemical methods. Physical activation involves activating the biochar with an oxidizing gas such as  $\text{CO}_2$ , steam, or their combination at relatively high temperatures (Aworn *et al.*, 2008). In chemical activation, the biochar is impregnated with a chemical agent such as  $\text{KOH}$ ,  $\text{NaOH}$ ,  $\text{K}_2\text{CO}_3$ ,  $\text{ZnCl}_2$ , and  $\text{H}_3\text{PO}_4$  and then it is heated in an inert atmosphere at

various temperatures (Gundogdu *et al.*, 2013).

More than 500000 tons of rice husk (RH) is produced annually in Iran as raw biomass (Abedi Koupai and Fathi, 2003). Unfortunately, most of this residue is burned, causing air pollution and human health problems. Therefore, it will be useful to consider the use of this material for producing applicable and suitable products, providing positive effects on the environment. The application of carbon-based material is significantly affected by its properties, which depend on the precursor type and preparation procedure (Rambabu *et al.*, 2013; Stals *et al.*, 2013). Therefore, knowing the characteristics of carbon-based materials is an important issue for selecting a suitable adsorbent to remove specified compounds. The first objective of this research was conversion of rice husk to biochar at different pyrolysis temperatures, activated carbon using steam,  $\text{KOH}$ , and both  $\text{KOH}$  and steam activation and also evaluation of their physicochemical characteristics. To our knowledge, there is limited information about application of biochar and activated carbon to sodium sorption. Our second objective was to consider the potential of the biochars and activated carbons to remove  $\text{Na}$ , as the main cation causing salinity, from saline waters.

## MATERIALS AND METHODS

### Preparation of Biochars and Activated Carbons

Rice husk (RH) was used as feedstock for biochar production. The RH was rinsed with boiling distilled water and oven-dried at  $105^\circ\text{C}$  for 24 h. The oven-dried RH was crushed and sieved to the particle size of less than 0.5 mm. The pyrolysis system consisted of a reactor with inlet and outlet devices allowing movement of gaseous flow through the sample. The reactor was placed in the electrical furnace with a programmable

temperature controller. A thermocouple was employed to measure the temperature in the reactor. The RH material was pyrolysed under inert  $N_2$  gas from room temperature to the desired carbonization temperature (400, 600, and 800 °C) at a heating rate of 10 °C min<sup>-1</sup> and held at the peak temperature for 2 h before cooling to room temperature. The biochars prepared at 400, 600, and 800 °C were denoted as RHB4, RHB6 and RHB8, respectively.

The RHB6 was selected to prepare the physically and chemically activated carbon. For the physical activation, water steam was selected as activation agent. A sub-sample of RHB6 was reheated under  $N_2$  gas from room temperature to 800 °C at a heating rate of 10 °C min<sup>-1</sup>. Then, the activation began by introducing water steam at 800 °C for 1 h. Later, the activated biochar was allowed to cool under  $N_2$  gas. The physically-activated carbon was denoted as RHBS.

For the chemical activation, KOH was selected as activation agent. A sub-sample of RHB6 was first impregnated with KOH. The ratio of KOH: biochar was 3:1 (w/w). The mixture was allowed to stand at room temperature for 24 h, and then oven-dried at 105 °C for 24 h. The dried sample was placed into reactor and heated under  $N_2$  gas at 800 °C for 1 h, and then cooled-down under  $N_2$  gas. The activated sample was washed several times with hot distilled water, and finally with cold distilled water until the pH of the filtrate was neutral. The washed sample was dried at 105 °C for 24 h. The chemically-activated carbon was denoted as RHBK.

For physiochemical activation, the RHBK was used. A sub-sample of RHBK was heated under  $N_2$  gas from room temperature up to 800 °C, then steam flow was injected into reactor for 1 h. Afterwards, the sample was cooled down under  $N_2$  gas. The physiochemically-activated carbon was denoted as RHBKS.

#### Characterization of Biochars and Activated Carbons

The prepared biochars and the activated carbons were characterized by several

techniques. The product yield was calculated as the weight ratio of final RH carbon-based sample to the initial-dried raw material. The ash of the samples was obtained by their oxidation under atmospheric condition in an electrical furnace at 800 °C for 4 h. Electrical conductivity (EC) and pH was measured by adding each sample to deionized water in a mass ratio of 1:100. The solution was shaken for 2 h and then filtered before measuring the pH and EC. A Metrohm 827 mV/pH-meter and a CC-501 Elmetron conductivity-meter were used for measuring the pH and EC, respectively.

The pH at which charge of the solid surface is zero is referred as zero point of charge ( $pH_{ZPC}$ ). To determine the  $pH_{ZPC}$  value of biochars and activated carbons, 0.1 g of each sample was introduced into 50 mL of 0.1 M  $KNO_3$  solution with initial pH range of 2-10 and was shaken for 24 h. After that, the sample was separated from solution and equilibrium pH values of the solution were measured with a pH-meter. The difference between initial and equilibrium pH was plotted against initial pH of the solution. The point at which the graph crossed the x-axis was noted as  $pH_{ZPC}$  value.

Quantities of surface acidic and basic functional groups of the carbon-based samples were determined by Boehm titration method (Cheung *et al.*, 2012). According to this method, 0.5 g of each sample was added separately to 50 mL of NaOH (0.1 M) and HCl (0.1 M), and shaken for 24 h. After the mixtures were separated, the basic and acidic filtrates were titrated with 0.1 M HCl and 0.1 M NaOH, respectively. The amount of total acidic and basic groups on the sample surface was estimated from the amount neutralized by NaOH and HCl solutions, respectively.

Physical characteristics of the samples were determined by  $N_2$  adsorption-desorption isotherm at -196°C using Belsorp mini II instrument. The BET surface area ( $S_{BET}$ ) was calculated by the Brunauer–Emmet–Teller (BET) method. The total pore volume ( $V_t$ ) was obtained by  $N_2$  adsorption at a relative pressure of 0.98. The complex



network of pores have been classified into micropores (diameter <2 nm), mesopores (diameter 2–50 nm), and macropores (diameter >50 nm). Micropore volume ( $V_{mic}$ ) was derived from the t-plot method. Pore-size distribution and mesopore volume ( $V_{mes}$ ) were determined by Barret-Joyner-Hanlenda (BJH) method.

The surface functional groups were recorded by Fourier Transform Infra-red (FTIR) spectra using JASCO FTIR-680 spectrophotometer, within the range of wave number of 400 to 4000  $cm^{-1}$ .

### Sodium Sorption of Biochars and Activated Carbons

Sodium sorption capacity was determined to compare sorption capacity of the biochar and activated carbons for cations. The Na sorption capacity was determined by adding 0.2 g of each sample to 25 mL of 0.2 M NaCl. The NaCl used in this experiment was of analytical grade. The mixture was shaken for 24 h. The solution was filtered using Whatman 42 filter paper and the Na concentration in the filtrated solution was measured using a Corning 410 flame photometer. The Na sorption capacity was calculated as follows:

$$q_e = \frac{(C_0 - C_e)V}{m} \quad (1)$$

Where,  $q_e$  ( $mg\ g^{-1}$ ) is the amount of sorbed Na at equilibrium,  $C_0$  ( $mg\ L^{-1}$ ) is initial

concentration of Na ion ( $mg\ L^{-1}$ ),  $C_e$  ( $mg\ L^{-1}$ ) is equilibrium concentration of Na,  $V$  (L) is the volume of the solution, and  $m$  (g) is mass of the sample.

To determine sorption isotherm, the initial molarity of NaCl solution ranged from 0.05 M to 0.3 M. For adsorption kinetic studies, 0.2 g of the selected adsorbent was added to 25 mL of 0.2 M NaCl and the mixture was shaken for varying amount of time. Then, the solution was filtered and Na concentration in the filtrated solution was determined. The amount of sorbed Na is described by equations (2) to (4) as follows:

$$\text{Pseudo-first order: } q_t = q_e (1 - e^{-k_1 t}) \quad (2)$$

$$\text{Pseudo-second order: } q_t = \frac{q_e^2 k_2 t}{1 + q_e k_2 t} \quad (3)$$

$$\text{Intra-particle diffusion: } q_t = k_i t^{0.5} - c \quad (4)$$

Where,  $q_t$  ( $mg\ g^{-1}$ ) is the amount of sorbed Na at time  $t$ ,  $q_e$  ( $mg\ g^{-1}$ ) is the amount of sorbed Na at equilibrium, and  $k_1$ ,  $k_2$ ,  $k_i$  and  $c$  are constants.

## RESULTS AND DISCUSSION

### Selected Properties of the Biochars and Activated Carbons

Selected properties of the biochars and activated carbons are shown in Table 1. The product yield of biochars decreased with rising the pyrolysis temperature due to large

**Table 1.** Selected properties of the studied biochars and activated carbons.

Sample	Yield (%)	Ash (%)	pH	EC ( $dS\ m^{-1}$ )
RHB4 <sup>a</sup>	46.8	32.8	8.2	0.07
RHB6 <sup>b</sup>	40.1	41.1	9	0.12
RHB8 <sup>c</sup>	35.4	43.1	10.1	0.14
RHBS <sup>d</sup>	32.6	46.8	10.1	0.21
RHBK <sup>e</sup>	28.2	11.5	9.2	0.26
RHBKS <sup>f</sup>	24.7	3.7	9.7	0.24

<sup>a</sup> Biochar prepared at 400 °C, <sup>b</sup> Biochar prepared at 600 °C, <sup>c</sup> Biochar prepared at 800 °C,

<sup>d</sup> Physically- activated carbon, <sup>e</sup> Chemically- activated carbon, <sup>f</sup>Physiochemically- activated carbon

amount of volatiles that could be easily released at higher temperatures. The product yield of activated carbons was lower compared to the biochars. This indicated that the activation agent reacted with carbon content of biochar and decreased its yield. Higher weight loss under activation with KOH was because of increasing the release of volatile products as a result of intensifying dehydration and elimination reactions (Tan *et al.*, 2008). The ash content of the biochars increased by increasing pyrolysis temperature. The amount of ash was higher in the biochar productions than the activated carbons produced by KOH agent. This is in agreement with the results found by Tay *et al.* (2009). The RHBKS had the lowest ash.

The pH of the biochars and activated carbons was in the range of 8.2-10.1. The higher pH for the biochars prepared at higher temperatures was probably due to the release of acidic surface groups during the pyrolysis (Mendez *et al.*, 2013). The EC value of the biochars and activated carbon varied from 0.07 to 0.26 dS m<sup>-1</sup>. This parameter was used to estimate total dissolved solids in the water sample. Overall, the EC of the biochars and activated carbons was low, which indicated that the amount of water-soluble ions in the prepared samples was low.

### Surface Chemistry

The pH<sub>ZPC</sub> is a very useful parameter that expresses surface charge of the adsorbent and its interactions with adsorbates. Net charge of the adsorbent under and above pH<sub>ZPC</sub> is positive and negative, respectively. All prepared samples had pH<sub>ZPC</sub> in the range of 6.8-8.5 (Table 2). The results indicated that pH<sub>ZPC</sub> of the samples depended on carbonization temperature and activation agent. Quantification of acidic and basic groups of the biochars and activated carbons are given in Table 2. All the samples, except RHB4, had more basic surface sites than acidic sites. The value of pH<sub>ZPC</sub>>7 confirmed the basic properties of the samples. Maximum total acidic surface groups belonged to RHB4 and declined with increasing carbonization temperature. According to Minkova *et al.* (2000), decomposition of the acidic groups at temperatures above 600 °C causes production of basic carbon-based materials. All activations produced basic activated carbons.

### Physical Characteristics

It is well known that surface area, porosity, and pore size distribution are the most important parameters for evaluating the sorption capacity of carbon-based material.

**Table 2.** Quantities of surface functional groups and pH<sub>ZPC</sub> of the biochars and activated carbons.

Sample	Acidic groups (mmol g <sup>-1</sup> )	Basic groups (mmol g <sup>-1</sup> )	pH <sub>ZPC</sub>
RHB4 <sup>a</sup>	1.21	0.34	6.8
RHB6 <sup>b</sup>	0.49	0.71	7.7
RHB8 <sup>c</sup>	0.30	0.64	8.5
RHBS <sup>d</sup>	0.46	0.69	7.8
RHBK <sup>e</sup>	0.59	0.92	7.1
RHBKS <sup>f</sup>	0.36	0.61	7.5

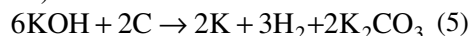
<sup>a</sup> Biochar prepared at 400 °C, <sup>b</sup> Biochar prepared at 600 °C, <sup>c</sup> Biochar prepared at 800 °C, <sup>d</sup> Physically- activated carbon, <sup>e</sup> Chemically- activated carbon, <sup>f</sup>Physiochemically- activated carbon

**Table 3.** Textural characteristics of the biochars and activated carbons.

Sample	$S_{\text{BET}}^a$ ( $\text{m}^2 \text{g}^{-1}$ )	$V_t^b$ ( $\text{cm}^3 \text{g}^{-1}$ )	$V_{\text{mic}}^c$ ( $\text{cm}^3 \text{g}^{-1}$ )	$V_{\text{mes}}^d$ ( $\text{cm}^3 \text{g}^{-1}$ )	$D_p^e$ (nm)
RHB4 <sup>f</sup>	32.6	0.029	0.015	0.014	3.49
RHB6 <sup>g</sup>	211.3	0.114	0.090	0.024	2.15
RHB8 <sup>h</sup>	202.4	0.104	0.080	0.024	2.06
RHBS <sup>k</sup>	317	0.175	0.136	0.039	2.21
RHBK <sup>l</sup>	2201	0.957	0.924	0.033	1.74
RHBKS <sup>m</sup>	1168.8	0.498	0.462	0.036	1.70

<sup>a</sup> BET surface area; <sup>b</sup> total pore volume; <sup>c</sup> micropore volume, <sup>d</sup> mesopore volume; <sup>e</sup> mean pore diameter. <sup>f</sup> Biochar prepared at 400 °C, <sup>g</sup> Biochar prepared at 600 °C, <sup>h</sup> Biochar prepared at 800 °C, <sup>k</sup> Physically- activated carbon, <sup>l</sup> Chemically- activated carbon, <sup>m</sup>Physiochemically- activated carbon

The physical properties of the biochars and activated carbons are given in Table 3. Raw rice husk material had very low surface area of  $1.43 \text{ m}^2 \text{g}^{-1}$ , and pyrolysis and activation increased it significantly. RHB4 had the least surface area ( $32.6 \text{ m}^2 \text{g}^{-1}$ ) and pore volume ( $0.029 \text{ cm}^3 \text{g}^{-1}$ ) among the biochars. By raising the carbonization temperature from 400 °C, the surface area and pore volume of biochars increased. This is probably because of the removal of higher amounts of volatiles compounds resulting from decomposition of major compounds of RH during the carbonization process. Our results indicated that the activation process improved development of pores and enhanced surface area of the biochars (Table 3). The RHBK showed a developed porous structure with  $S_{\text{BET}}$  of  $2201 \text{ m}^2 \text{g}^{-1}$  and  $V_t$  of  $0.96 \text{ cm}^3 \text{g}^{-1}$ . The reaction between KOH and carbon could be as follows (Deng *et al.*, 2010):



It is assumed that KOH is reduced to metallic K during the carbonization process. When activation temperature reaches the boiling point of K ( $760^\circ\text{C}$ ), K is diffused into the layer of carbon and causes formation of new pores in the carbon structure, which increases porosity and surface area. According to Table 3, KOH agent, compared to steam, produced smaller

mean pore diameter. Wu *et al.* (2005) reported that activation with KOH produced mainly micropores and a narrower pore size distribution. Compared to steam, KOH agent significantly increased surface area and pore volume, although both RHBS and RHBK were prepared in the same carbonization and activation temperatures. The high ash content of RHB6 (Table 1) decreased the reaction of steam with organic carbon and, therefore, development of pore structure of physically-activated carbon was relatively low. Physiochemical activation was not satisfactory in development of pore structure (Table 3). The surface area and pore volume of RHBKS decreased as compared to RHBK. This was probably because of developing pore structures in the RHBK under further activation causing the walls of the pores to become very thin and collapse, consequently, producing pores too small to be measured by the BET analysis (Wang *et al.*, 2013). This caused significant reduction in the surface area and pore volume of RHBKS.

Micropore volume occupied about 78%, 96%, and 93% of total pore volume of RHBS, RHBK and RHBKS, respectively (Table 3). This supported the idea that the prepared activated carbons were microporous material. The shape of  $\text{N}_2$  adsorption-desorption isotherms of the samples (Figure 1) supports that the majority

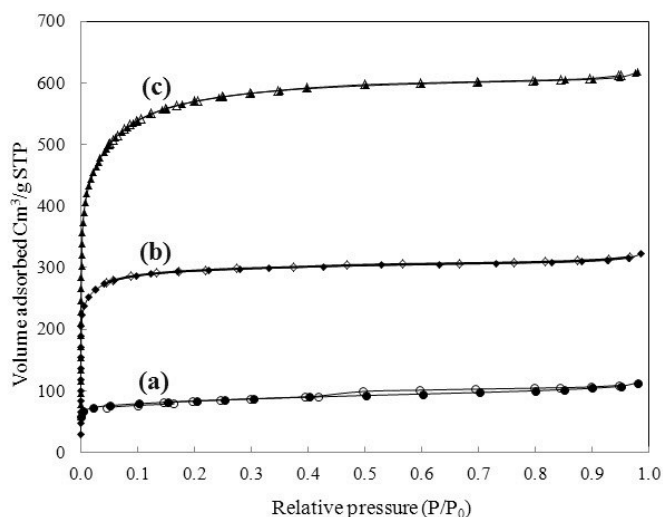


**Figure 1.**  $N_2$  adsorption-desorption isotherms of a) RHBS, b) RHBKS, and c) RHBK.

of pores were micropores. According to IUPAC classification, the isotherms are type I, indicating mostly a microporous structure.

Pore size distributions of the biochars and activated carbons showing the internal structure of samples are presented in Figure 2, which shows that the pore size distributions were dependent on the carbonization temperature and activation agent. For all the samples, micropores were the dominant pores. The shift of mean pore

diameter to smaller values for RHBK and RHBKS indicates that chemical and physiochemical activation promotes the creation of new micropores. The close knee of isotherm shown in Figure 1 clearly proves the narrow microporous nature of RHBK and RHBKS.

### FTIR Analysis

Surface functional group is another

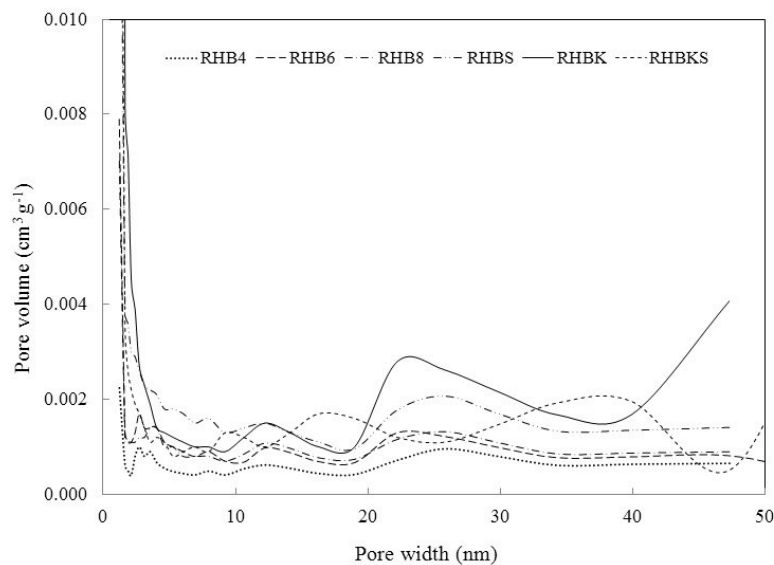


**Figure 2.** Pore size distribution of biochars and activated carbons.





effective parameter on adsorption capacity of the adsorbent. FTIR is perhaps the most powerful tool for identifying type of the functional groups. Figure 3 shows the FTIR spectra of the prepared biochars and activated carbons. The intensity of functional groups for RHB4 was more than the other biochars. The spectra of the RHB4 were characterized by several major peaks. Broad peak at  $3443\text{ cm}^{-1}$  is typically attributed to hydroxyl groups (O-H). The strong peaks located at  $469\text{ cm}^{-1}$ ,  $803\text{ cm}^{-1}$  and  $1098\text{ cm}^{-1}$  are ascribed to bending vibration, symmetric stretching and asymmetric stretching of Si-O bonds (Guo and Rockstraw, 2007; Mohamed, 2004). The presence of these peaks was due to the existence of silica. The peak at  $1382\text{ cm}^{-1}$  can be assigned to C-O stretching vibration. The strong peak at  $1613\text{ cm}^{-1}$  can be attributed to C=C stretching vibration. The weak stretching vibration of C-H bond is visible as a peak at  $2924\text{ cm}^{-1}$ . Results showed that the spectra of RHB4, RHB6 and RHB8 were very similar to each other and intensities of these bands decreased with change of temperature from  $400\text{ }^{\circ}\text{C}$  to  $800$

$^{\circ}\text{C}$ . The peak at  $2924\text{ cm}^{-1}$  disappeared at higher temperatures, indicating organic hydrocarbons were decomposed into methane, carbon dioxide, and other gases or aromatic structures (Lu et al., 2013). The trend in spectra for RHBS was similar to RHB6. The additional peak appeared at  $2355\text{ cm}^{-1}$  which can be associated with  $\text{C}=\text{O}$  in ketene group (Gaur et al., 2006). Similar results were reported by El-Hendawy (2006) in a study on steam-activated carbon prepared from date pits. Significant differences in intensity of peak for RHBK were noted. Sharp peak located at  $1098\text{ cm}^{-1}$  was decreased intensively and the peak located at around  $470\text{ cm}^{-1}$  was disappeared. This result indicates that KOH agent could decrease silica content of RHB. It suggests that various surface groups formed on carbon could be influenced by the activation agent.

### Sodium Sorption Capacity

The Na sorption capacity of the prepared samples was tested and the results are

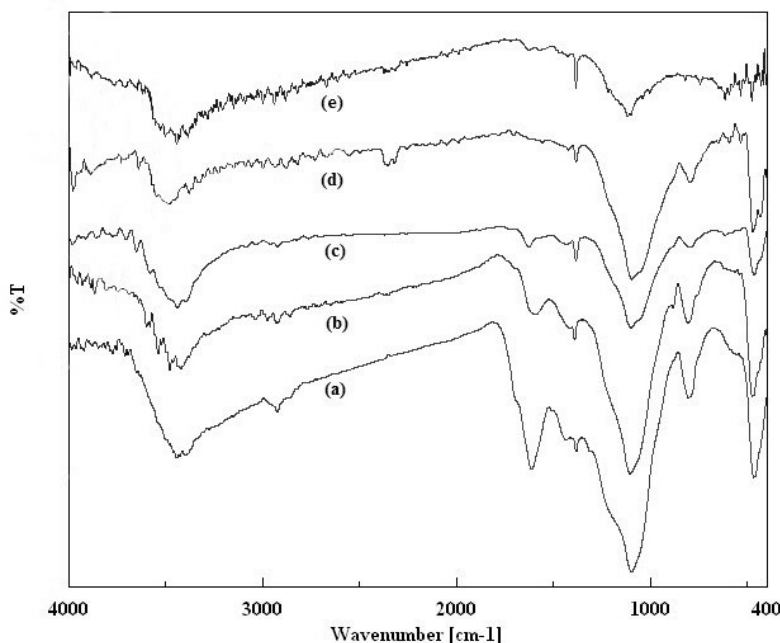


**Figure 3.** FTIR of a) RHB4, b) RHB6, c) RHB8, d) RHBS and e) RHBK.

presented in Table 4. The sorption capacity was in the range of 35.2-134.2 mg g<sup>-1</sup>. Activation increased Na sorption capacity of biochar and RHBK, had the highest tendency for Na sorption. In general, sorption capacity of the carbon-based materials is influenced by such characteristics as surface functional groups, surface area, pore volume, and pore size distribution. Correlation between Na capacity and acidic surface functional groups and textural characteristics of the prepared samples are shown in Figure 4. Although the more acidic groups can enhance ion exchange, specific relation between surface acidity and Na sorption was not observed. The greatest acidic group belonged to RHB4; however, RHB4 had the lowest sorption capacity. Also, FTIR spectra (Figure 3) did not present any special surface group, which indicates probability of involvement between Na ion and surface group in the sorption process.

Figures 4b and 4c show an increase in Na sorption capacity with increasing surface

**Table 4.** Na sorption capacity of the biochars and activated carbons.

Sample	Na sorption capacity (mg g <sup>-1</sup> )
RHB4	35.2
RHB6	60.8
RHB8	53.9
RHBS	73.5
RHBK	134.2
RHBKS	102.1

area and pore volume. High surface area increases migration of ions from the bulk solution to the surface of the adsorbent. Na sorption had an approximate linear relation with  $S_{\text{BET}}$  and  $V_t$ . The  $R^2$  values of linear relation were 0.932 and 0.938, respectively, indicating that textural properties of the prepared adsorbents were the key factor in Na sorption in our experiments. The sorption capacity of carbon porous materials depends on the accessibility of molecules to reach the inner surface of the adsorbent, which

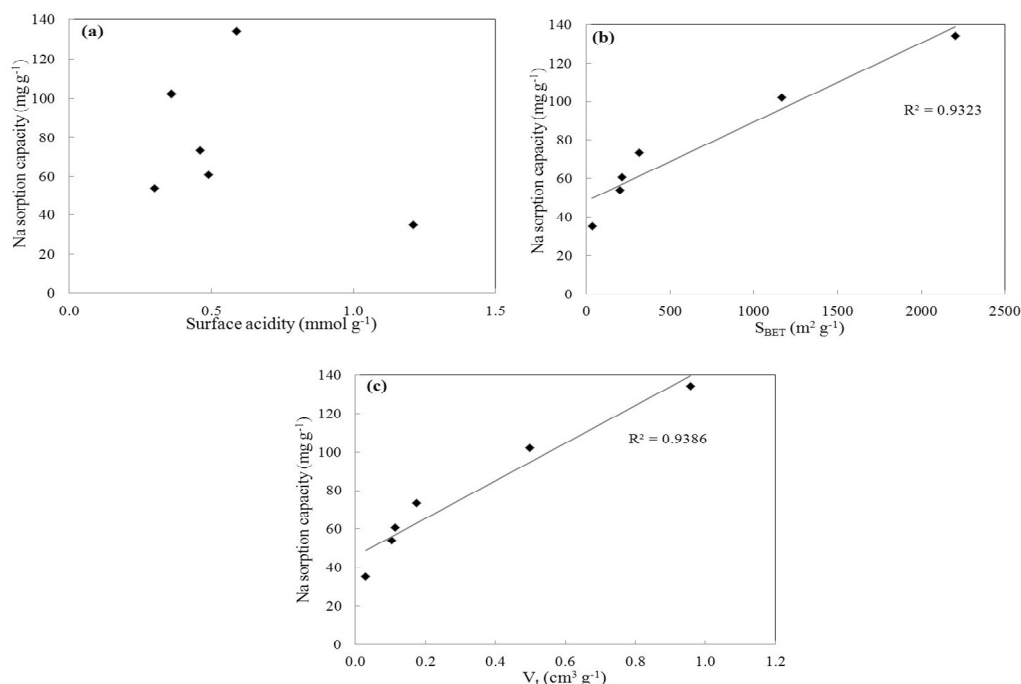


**Figure 4.** Sodium sorption capacity of the adsorbents, textural structures, and surface acidity properties.



depends on their size. Pore diameter, being larger than the size of adsorbate, improves accessibility to the internal surface of the adsorbent materials. Rohani and Entezari (2012) reported that activated carbon with mean pore size of about 2.2 nm was a suitable adsorbent for removing P-nitrophenol with a size of 0.75 nm. The iodine element with a size of 0.56 nm is greatly adsorbed into micropores (Gundogdu *et al.*, 2013). The hydrated ionic radius of Na has been estimated to be about 0.178 nm (Kiriukhin and Collins, 2002). According to the size of Na ion, the micropores could act as effective pores to adsorb this cation. As the total pore volume increased, micropores volume also increased (Table 3). The RHBK which was the most effective adsorbent for Na sorption had the highest percentage of micropore volume.

### Sorption Isotherm and Kinetics Study

RHBK, as the most effective adsorbent,

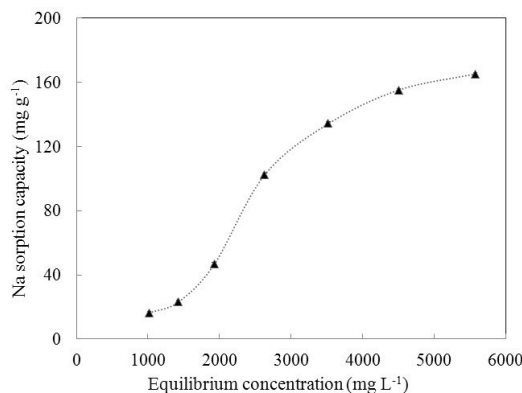


Figure 5. Sorption isotherm of Na on RHBK.

was selected for more studies. Figure 5 shows the amount of sorbed Na versus equilibrium concentration. The amount of Na sorbed by RHBK increased from 16.4 to 165.1 mg g<sup>-1</sup> as the initial Na concentration increased from 0.05 to 0.3 M, probably due to a greater concentration gradient and diffusive movement of Na ions toward and/or into the adsorbent at higher Na concentrations in solution.

Figure 6 shows the effect of contact time on the amount of Na sorbed by RHBK. Sorption kinetics of Na on the RHBK adsorbent was studied by employing pseudo-first order, pseudo-second order and intra-particle diffusion models. Table 5 shows the obtained constants for kinetics models used in this study. Coefficient of determination (R<sup>2</sup>) and standard estimation error (SEE) were used for evaluation of the models. There was a good agreement between experimental data and the calculated Na sorbed values according to pseudo-first order and intra-particle diffusion models.

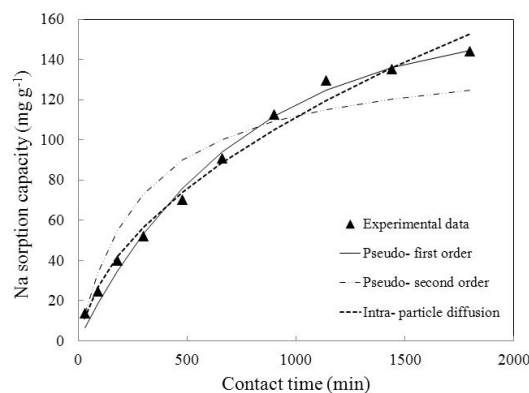


Figure 6. Sorption kinetics of Na on RHBK.

Table 5. Parameters of kinetic models for Na sorption by RHBK.

Pseudo-first order		Pseudo-second order		Intra-particle diffusion	
$q_e$ (mg g <sup>-1</sup> )	157.99	$q_e$ (mg g <sup>-1</sup> )	144.94	$K_i$ (mg g <sup>-1</sup> min <sup>-0.5</sup> )	3.84
$K_1$ (min <sup>-1</sup> )	0.0014	$K_2$ (g mg <sup>-1</sup> min <sup>-1</sup> )	0.000023	$C$ (mg g <sup>-1</sup> )	10.07
<sup>a</sup> R <sup>2</sup>	0.995	R <sup>2</sup>	0.945	R <sup>2</sup>	0.993
<sup>b</sup> SEE	4.87	SSE	15.97	SSE	5.91

<sup>a</sup> Coefficient of determination, <sup>b</sup> Standard Estimation Error

Results indicated that intra-particle diffusion was involved in the sorption process. Pseudo-second order model, which was indicative of a possible chemisorption process, had the lowest agreement with experimental data and was not satisfactorily fitted to the data.

## CONCLUSIONS

Rice husk biochars were prepared at three carbonization temperatures (400 (RHB4), 600 (RHB6), and 800 °C (RHB8)). Results showed that surface area and porosity of RHB4 were very low and increased significantly by increasing the carbonization temperature; while the surface acidic functional groups of the biochar decreased. Activated carbon was derived from the biochar using steam, KOH, and both agents. The activation process changed the physiochemical properties such as specific surface area, porosity, and surface functional groups. The high ash content of rice husk caused the reaction of steam with organic carbon and, therefore, the development of pore structure of physically-activated carbon was relatively low. Potassium hydroxide agent increased surface area, total pore volume, and micropores' volume of the biochar significantly and decreased its ash content. Sorption capacity for Na by the prepared samples was evaluated. Chemically-activated carbon had the highest sorption capacity. The results showed that Na sorption increased with increasing surface area and pore volume. Pseudo-first order and intra-particle diffusion models appeared to be suitable to describe the sorption kinetic data. Conversion of RH to biochar and activated carbon offers a solution for minimizing agricultural wastes volume and producing valuable adsorbents to improve water quality.

## REFERENCES

1. Abedi Koupai, J. and Fathi, M.A. 2003. Mechanical Properties of Concrete Canal Lining Containing Rice Husk Ash in Sulfate Environments. *J. Water Soil Sci.*, 7: 13-17.
2. Aghakhani, A., Mousavi, S.F., Mostafazadeh-Fard, B., Rostamian, R. and Seraji, M. 2011. Application of Some Combined Adsorbents to Remove Salinity Parameters from Drainage Water. *Desalination*, **275**: 217-223.
3. Aworn, A., Thiravetyan, P. and Nakbanpote, W. 2008. Preparation and Characteristics of Agricultural Waste Activated Carbon by Physical Activation Having Micro- and Mesopores. *J. Anal. Appl. Pyrol.*, **82**: 279-285.
4. Cheung, W. H., Lau, S. S. Y., Leung, S. Y., Ip, A. W. M. and McKay, G. 2012. Characteristics of Chemical Modified Activated Carbons from Bamboo Scaffolding. *Chinese J. Chem. Eng.*, **20**: 515-523.
5. Deng, H., Li, G., Yang, H., Tang, J. and Tang, J. 2010. Preparation of Activated Carbons from Cotton Stalk by Microwave Assisted KOH and K<sub>2</sub>CO<sub>3</sub> Activation. *Chem. Eng. J.*, **163**: 373-381.
6. El-Hendawy, A. N. A. 2006. Variation in the FTIR Spectra of a Biomass under Impregnation, Carbonization and Oxidation Conditions. *J. Anal. Appl. Pyrol.*, **75**: 159-166.
7. Gasco, G., Mendez, A. and Gasco, J. M. 2005. Preparation of Carbon-based Adsorbents from Sewage Sludge Pyrolysis to Remove Metals from Water. *Desalination*, **180**: 245-251.
8. Gaur, V., Sharma, A. and Verma, N. 2006. Preparation and Characterization of ACF for the Adsorption of BTX and SO<sub>2</sub>. *Chem. Eng. Process.*, **45**: 1-13.
9. Gundogdu, A., Duran, C., Senturk, H. B., Soylak, M., Imamoglu, M. and Onal, Y. 2013. Physicochemical Characteristics of a Novel Activated Carbon Produced from Tea Industry Waste. *J. Anal. Appl. Pyrol.*, **104**: 249-259.
10. Guo, Y. and Rockstraw, D. A. 2007. Activated Carbons Prepared from Rice Hull by One-step Phosphoric Acid Activation. *Micropor. Mesopor. Mater.*, **100**: 12-19.
11. IUPAC. 1972. Manual of Symbols and Terminology. *Pure Appl. Chem.*, **31**: 587.
12. Jiang, T. Y., Jiang, J., Xu, R. K. and Li, Z. 2012. Adsorption of Pb(II) on Variable Charge Soils Amended with Rice-straw Derived Biochar. *Chemosphere*, **89**: 249-256.
13. Kiriukhin, M. Y. and Collins, K. D. 2002. Dynamic Hydration Numbers for Biologically Important Ions. *Biophys. Chem.*, **99**: 155-168.
14. Kolodynska, D., Wnetrzak, R., Leahy, J.J., Hayes, M. H. B., Kwapiński, W. and Hubicki, Z. 2012. Kinetic and Adsorptive Characterisation of Biochar in Metal Ions Removal. *Chem. Eng. J.*, **197**: 295-305.



15. Lu, X., Jiang, J., Sun, K., Xie, X. and Hu, Y. 2012. Surface Modification, Characterization and Adsorptive Properties of a Coconut Activated Carbon. *Appl. Surf. Sci.*, **258**: 8247-8252.
16. Lu, H., Zhang, W., Wang, S., Zhuang, L., Yang, Y. and Qiu, R. 2013. Characterization of Sewage Sludge-derived Biochars from Different Feedstocks and Pyrolysis Temperatures. *J. Anal. Appl. Pyrol.*, **102**: 137-143.
17. Mendez, A., Terradillos, M. and Gasco, G. 2013. Physicochemical and Agronomic Properties of Biochar from Sewage Sludge Pyrolysed at Different Temperatures. *J. Anal. Appl. Pyrol.*, **102**: 124-130.
18. Minkova, V., Marinov, S.P., Zanzi, R., Bjornbom, E., Budinova, T., Stefanova, M. and Lakov, L. 2000. Thermochemical Treatment of Biomass in a Flow of Steam or in a Mixture of Steam and Carbon Dioxide. *Fuel Process. Technol.*, **62**: 45-52.
19. Mohamed, M. M. 2004. Acid Dye Removal: Comparison of Surfactant-modified Mesoporous FSM-16 with Activated Carbon Derived from Rice Husk. *J. Colloid Interf. Sci.*, **272**: 28-34.
20. Mousavi, S. F., Mostafazadeh-Fard, B., Farkhondeh, A. and Feizi, M. 2009. Effects of Deficit Irrigation with Saline Water on Yield, Fruit Quality and Water Use Efficiency of Cantaloupe in an Arid Region. *J. Agric. Sci. Technol.*, **11**: 469-479.
21. Pehlivan, E. and Cetin, S. 2008. Application of Fly Ash and Activated Carbon in the Removal of  $\text{Cu}^{2+}$  and  $\text{Ni}^{2+}$  Ions from Aqueous Solutions. *Energ. Source., A*, **30**: 1153-1165.
22. Rambabu, N., Azargohar, R., Dalai, A. K. and Adjaye, J. 2013. Evaluation and Comparison of Enrichment Efficiency of Physical/Chemical Activations and Functionalized Activated Carbons Derived from Fluid Petroleum Coke for Environmental Applications. *Fuel Process. Technol.*, **106**: 501-510.
23. Rohani Bastami, T. and Entezari, M. H. 2012. Activated Carbon from Carrot Dross Combined with Magnetite Nanoparticles for the Efficient Removal of P-nitrophenol from Aqueous Solution. *Chem. Eng. J.*, **210**: 510-519.
24. Stals, M., Vandewijngaarden, J., Wrbel-Iwaniec, I., Gryglewicz, G., Carleer, R., Schreurs, S. and Yperman, J. 2013. Characterization of Activated Carbons Derived from Short Rotation Hardwood Pyrolysis Char. *J. Anal. Appl. Pyrol.*, **101**: 199-208.
25. Tan, I. A., Ahmad, A. L. and Hameed, B. H. 2008. Preparation of Activated Carbon from Coconut Husk: Optimization Study on Removal of 2,4,6-Trichlorophenol Using Response Surface Methodology. *J. Hazard. Mater.*, **153**: 709-717.
26. Tay, T., Ucar, S. and Karagoz, S. 2009. Preparation and Characterization of Activated Carbon from Waste Biomass. *J. Hazard. Mater.*, **165**: 481-485.
27. Wang, R., Amano, Y. and Machida, M. 2013. Surface Properties and Water Vapor Adsorption-desorption Characteristics of Bamboo-based Activated Carbon. *J. Anal. Appl. Pyrol.*, **104**: 667-674.
28. Wu, F. C., Tseng, R. L. and Juang, R. S. 2005. Comparisons of Porous and Adsorption Properties of Carbons Activated by Steam and KOH. *J. Colloid Interf. Sci.*, **283**: 49-56.
29. Zhang, G., Zhang, Q., Sun, K., Liu, X., Zheng, W. and Zhao, Y. 2011. Sorption of Simazine to Corn Straw Biochars Prepared at Different Pyrolytic Temperatures. *Environ. Pollut.*, **159**: 2594-2601.

## خصوصیات و ظرفیت جذب سدیم زغال زیستی و کربن فعال تهیه شده از شلتوک برنج

ر. رستمیان، م. حیدرپور، س.ف. موسوی و م. افیونی

### چکیده

زغال زیستی و کربن فعال به عنوان مواد متخلخل کربنی کاربرد وسیعی در محیط زیست دارند. در مطالعه حاضر از شلتوک برنج برای تهیه زغال زیستی تهیه شده در دماهای ۴۰۰، ۶۰۰ و ۸۰۰ درجه سلسیوس تحت پیرولیز ساده و کربن فعال شده فیزیکی با بخار آب، کربن فعال شده شیمیایی با هیدروکسید پتاسیم (KOH)، و کربن فعال شده شیمیایی- فیزیکی با بخار آب و KOH استفاده شد. خصوصیات مواد کربنی تهیه شده با استفاده از ایزوترم جذب و واجذب گاز نیتروژن، طیف سنجی مادون قرمز با تبدیل فوری (FTIR) و تیتراسیون بوهم بررسی شد. نتایج نشان داد که دمای کربن سازی و عامل فعال سازی تأثیر زیادی بر خصوصیات ماده کربنی تولید شده دارد. کربن فعال شده شیمیایی بیشترین سطح ویژه ( $2201 \text{ m}^2/\text{g}$ ) و حجم حفره ها ( $0.96 \text{ cm}^3/\text{g}$ ) را داشت. غلظت زیاد سدیم مهترین عامل محدود کننده استفاده از منابع آب با کیفیت نامطلوب در نواحی خشک و نیمه خشک می باشد. بنابراین، ظرفیت جذب سدیم مواد کربنی تهیه شده مورد بررسی قرار گرفت. با افزایش سطح ویژه و حجم حفره ها، میزان جذب سدیم افزایش می یابد. کربن فعال شده شیمیایی بیشترین ظرفیت جذب سدیم ( $134/2$  میلی گرم بر گرم) را به خود اختصاص داد. داده های سینتیک جذب به خوبی از معادلات شبه مرتبه اول و پخشیدگی درون ذره ای پیروی کرد.